# Solid Materials with Near-Infrared-Induced Fluorescence Modulation

*Jaume Ramon Otaegui, Pau Rubirola, Daniel Ruiz-Molina, Jordi Hernando,* and Claudio Roscini**

J. Ramon Otaegui, J. Hernando

Departament de Química, Universitat Autònoma de Barcelona, 08193 Cerdanyola del Vallès, Spain

e-mail: jordi.hernando@uab.cat

P. Rubirola, D. Ruiz-Molina, C. Roscini

Catalan Institute of Nanoscience and Nanotechnology (ICN2), CSIC and The Barcelona Institute of Science and Technology, Campus UAB, Bellaterra, 08193 Barcelona, Spain

e-mail: claudio.roscini@icn2.cat

**Keywords**: fluorescence, near-infrared, switchable fluorescent materials, photothermal effect, rewritable devices

**Abstract.** Solid molecular materials that modulate their luminescent properties upon irradiation are typically based on photochromic dyes. Despite these are potentially interesting for applications such as anticounterfeiting, bioimaging, optical data storage, and writable/erasable devices, key features are preventing their use in marketable products: the lack of straightforward strategies to obtain near infrared radiation (NIR)-responding photochromic dyes and the dramatic response modification these molecules suffer in solids. Herein we report a photochrome-free approach to achieve solid materials, whose luminescence modulation is induced by NIR radiation. This strategy is based on the capacity of phase change materials (PCMs) to modify the emission properties of fluorescent dyes upon photothermally-induced interconversion between their solid and liquid states. We illustrate the preparation of several NIR-responsive thermofluorochromic materials of high fatigue resistance and non-destructive

readout, and extend this approach to different commercially available dyes, taking advantage of distinct fluorescence modulation mechanisms, providing, thus, colour tuneability. The modulation response is straightforwardly tuned by simply varying the irradiation power density, the gold nanoshell concentration and/or the PCM type. This tuneability allowed us to accomplish NIR-activated multistate thermofluorochromic materials and fast/slow/irreversible responses in NIR-writings/drawings of good spatial resolution, which could be of interest for barcodings, anticounterfeiting technologies and (re)writable devices.

## 1. Introduction

Light is a clean, non invasive and tuneable stimulus that allows the properties of molecules and materials to be remotely controlled in a reversible manner with remarkable time and spatial resolution.[1–8] Of particular interest are luminescent materials that undergo emission modulation upon irradiation,[9–12] which are exploited in high-density data storage[13,14] and information processing,[15] white light generation,[16] (bio)sensing and imaging,[17–20] anti-counterfeiting technologies,[21,22] and photowritable/erasable fluorescent inks,[23] among other areas. For many of these applications, the use of near-infrared radiation (NIR) to achieve luminescence modulation would be highly beneficial; e.g., to reach higher penetration depths with lower photodamage for (bio)imaging probes,[18,24] or to develop advanced security inks for anti-counterfeiting.[25]

Currently, most common methodologies applied to achieve fluorescence modulation are based on the reversible interconversion of photochromic dyes.[9,10,11–18,19–21] However, these systems suffer from important drawbacks that are limiting their application in commercial products. On one hand, the interconversion of photochromic dyes are generally based on isomerisation processes that involve large polarity and geometrical changes, which are often detrimentally affected by the surrounding matrix when these compounds are transferred from solution to the solid state. This is especially the case for photoswitchable luminescent materials based on T-type photochromes,[26] for which novel strategies are being developed to favour dye (photo)isomerisation in solid matrices (e.g., by covalently attaching bulky moieties to increase the surrounding free volume;[22],[27] or by using photoisomersable compounds with minimal conformational changes[26,28]). On the other hand, photochromic dyes typically operate under highly energetic UV or visible radiation (e.g., spiropyrans) which contributes significantly to fast dye degradation.[29] Actually, making photochromic compounds sensitive to NIR radiation still remains a challenge that requires intricate synthetic procedures[30–33] and/or multiphoton

excitation under high irradiation powers.[34–40] As such, their incorporation into more complex systems to attain NIR-induced luminescence modulation has been largely hampered to date.

As an alternative to photochromic-based systems, we report herein a conceptually different strategy to obtain NIR-driven fluorescence modulation in the solid state, which takes advantage of: (a) the recent discovery by us[41–43] and others[44–47] that the emission of selective dyes dispersed in phase change materials (PCMs) can be thermally varied upon solid-to-liquid interconversion; and (b) the photothermal effects generated by selective (nano)structures under NIR irradiation, which have already been employed to light-trigger PCM melting for drug delivery[48] and energy saving[49] and storage[50] purposes. In this work we aim to merge these two concepts to develop a novel, straightforward and universal methodology toward NIR-responsive thermofluorochromic materials, with which a variety of different NIR-induced fluorescence modulation schemes could be obtained by simply combining three essential components: fluorescent dyes, PCMs capable of altering the properties of the emitters upon interconversion between their solid and liquid states, and NIR-absorbing noble metal nanoparticles[51] (NMNPs) that photothermally-induce the phase transition of the PCMs under irradiation (Figure 1a). With this aim, new mechanisms for PCM-based fluorescence modulation have been developed, which have been proven to be vastly versatile and tuneable as well as operate under NIR-induced photothermal heating for the preparation of light-responsive emissive materials.

The advantages of our strategy for the preparation of NIR-responsive luminescent materials are expected to be multifold. On one hand, it counts on the photoactivity of NMNPs, which present large absorptivities, photostability and spectral tuneability.[51] As such, they can be designed to selectively respond to low-power NIR radiation while showing negligible absorption in the visible region where the material emits, thus preventing unwanted photophysical and photochemical processes that may be observed when attempting light-induced fluorescence modulation with photochromes (e.g., photodegradation,[52] destructive

readout,[53] emission quenching). On the other hand, it can be applied to readily available fluorophores and PCMs without the need for tedious synthetic modifications. Finally, by judiciously selecting the nature of these components and, if necessary, of auxiliary additives, it can be generalised to a large number of fluorescent molecules, thereby providing with a universal strategy towards thermofluorochromic materials with finely tuneable NIR-induced fluorescence modulation difficult to accomplish using the current methodologies based on T-type photochromes.

**- Insert Figure 1 here -**

## 2. Results and discussion

### 2.1 NIR-induced modulation of emission through PCMs transition: proof of concept.

To validate our approach, we first focused on developing a solid material that undergoes NIR-induced luminescence modulation based on a well-known case of environment-dependent emission: fluorescent molecular rotors, i.e., conformationally flexible emitters whose luminescence quantum yield ($\Phi_{em}$) increases with the rigidity of the surrounding medium.[54] When dispersed in a PCM, their emission should therefore abruptly decrease upon solid-to-liquid transition, as recently proven thermally for polydiphenylacetylenes.[44] Herein we aim to demonstrate that such behaviour can also be induced with NIR light in the absence of external heat by taking advantage of the photothermal effects generated by NMNPs. In particular, we considered the use of gold nanoshells (AuNSs), as they produce intense photothermal heating upon plasmon excitation with NIR radiation while showing weak absorption in the visible spectral region.[55,56] Accordingly, water-dispersible AuNSs of 92 ± 23 nm in diameter were synthesised using a reported procedure,[57] which displayed maximum extinction at $\lambda_{ext,max}$ = 890 nm (Figures 1b and 1c).

As a fluorescent molecular rotor, we selected the commercial dye {[5′-(*p*-hydroxyphenyl)-2,2′-bithienyl-5-yl]-methylidene}-propanedinitrile (**NIAD-4**, Figure 2a),[58] which shows a dramatic reduction of $\Phi_{em}$ in organic solvents of decreasing viscosity.[59] Actually, when dissolved in 1-tetradecanol (TdOH, 2.4 $10^{-3}$ wt%), an organic PCM with relatively low melting temperature ($T_m$ = 37.7 ºC),[60] we registered a clear 10-fold decrease in fluorescence emission intensity for **NIAD-4** when heating from 20 ºC to 50 ºC ($\Delta F$ = -89.6%, Figure 2b and Table S1). Because negligible changes in absorption were concomitantly observed (Figure S1), this could be mainly ascribed to the softening of the surrounding matrix upon melting and, hence, the activation of the radiationless decay pathways of the dye due to increased conformational flexibility.

**- Insert Figure 2 here -**

To exploit this thermal response for the preparation of NIR-responsive thermofluorochromic solid materials, we successively casted an aqueous suspension of AuNSs (340 μg $mL^{-1}$) and a liquid melt of **NIAD-4** in TdOH (2.4 $10^{-3}$ wt%) onto a porous cellulose-based paper (**NIAD-4/TdOH-AuNS@paper**). This led to the adsorption of AuNSs to the cellulose microfibers (13 μg $cm^{-2}$) and, upon cooling, the physical entrapment of the **NIAD-4**/TdOH mixture within the substrate (Figure S2). As a result, an uniformly coloured paper was obtained that preserved both the thermal properties of the phase change material (Figure S3) and the characteristic orange emission of the fluorophore ($\lambda_{em,max}$ = 620 nm, Figures 2c and 2d). In addition, the cellulose paper embedding the NIR-responsive thermofluorochromic mixture did not leak the adsorbed PCM when heated above its melting point, thus preserving its integrity upon successive heating-cooling cycles. Interestingly, when this material was irradiated with a cw NIR laser ($\lambda_{exc}$ = 830 nm, 10.6 mW $mm^{-2}$), a prompt loss of fluorescence was observed locally around the illuminated spot resembling the behaviour measured under external heating, which

could be rapidly reverted in the dark at room temperature ($\Delta F$ = -75.9%, Figures 2c and 2d, and Table S1). The initial fluorescence of NIAD-4 observed in the non-irradiated **NIAD-4/TdOH-AuNS@paper** was the consequence of the rigidity of the TdOH trapped within the paper fibers, which favoured the radiative pathway of the dye. NIR irradiation caused the local melting of TdOH and thus the softening of the surrounding medium of NIAD-4. In these conditions the dye loses the energy of the electronically excited state decaying through non-radiative paths, decreasing its fluorescence intensity. Once the irradiation is stopped, the TdOH turns back to the solid state and the NIAD-4 fluorescence is recovered. As this phenomenon was not registered for similar samples prepared without AuNSs, we ascribed the NIR-triggered emission modulation found for **NIAD-4/TdOH-AuNS@paper** to the photothermally-induced solid-to-liquid transition of its PCM (Figure S4). Again, no PCM leakage was detected in the irradiated area, thus indicating that the mixture was properly encapsulated within the cellulose paper fibres. The actual melting of the PCM was further proven by measuring the temperature achieved at the irradiated spot of **NIAD-4/TdOH-AuNS@paper** with an infrared probe, which raised up to *ca*. 65 ºC under cw NIR light. Although this value is averaged over all the illuminated area and, hence, is a lower limit of the actual temperatures reached in the vicinity of the gold nanostructures, it unambiguously demonstrates their capacity of photothermally melting TdOH (and even higher-$T_m$ PCMs) at NIR intensities that are considerably inferior than those required for inducing multiphoton operation of regular photochromes.[34–40]

Detailed analysis of the behaviour of **NIAD-4/TdOH-AuNS@paper** uncovered other additional advantages of our approach towards NIR-driven emission modulation. First, multiple consecutive cycles (up to 100) of light-induced fluorescence modulation could be measured without apparent degradation by repeatedly switching on and off the NIR source (Figure 2e), which demonstrates the large fatigue resistance of our switchable materials. Second, by decoupling dye and AuNS photoresponses, destructive readout[53] was prevented and, as such, no variation of the emissive state of the material was observed when monitoring the

fluorescence signal of **NIAD-4** upon prolonged UV or visible illumination (Figure 2f). Moreover, large, clear-cut emission changes were registered by switching on/off the NIR radiation, which simply relied on the capacity of altering fluorophore properties upon solid-to-liquid interconversion of the surrounding medium. Based on these features, the photothermally-sensitive paper substrates developed allow for writing patterns upon NIR irradiation that form and erase nearly instantaneously (Video S1).

**2.2 Generalisation of NIR-induced fluorescence modulation in PCMs.**

To explore the general scope of our methodology toward NIR-responsive thermofluorochromic materials, we considered the use of other fluorescence modulation mechanisms and common emitters that can be either commercially purchased or easily synthesised. For this, we inspired on our previous discovery that PCMs can selectively trigger chromophore aggregation upon solidification[41,43] and, as such, induce fluorescence modification via upconversion[41] and excimer emission.[43,45] This is due to the more limited solubility of these dyes in the PCMs when they are in their solid state. Aiming to expand the portfolio of PCM-controllable luminescence switching processes, three other fluorescence modulation mechanisms based on bi- (or multi-) molecular interactions were investigated herein: (a) aggregation-induced emission (AIE), which we assayed for the well-known AIE dye tetraphenylethene (**TPE**);[61] (b) aggregation-caused quenching (ACQ), which was tested for Rhodamine B (**RhB**);[42] and (c) photoinduced electron transfer (PET), for which we exploited the well-established ability of electron-donating aromatic amines (e.g. dimethylaniline, **DMA**) to quench the fluorescence of electron-accepting perylenebisimide fluorophores (e.g. *N*,*N*'-bis-(*sec*-butyl)-1,6,7,12-tetra-(4-*tert*-butylphenoxy)perylene-3,4:9,10-tetracarboxylic diimide, **PTDI**) via PET (Scheme S1).[62] It must be noted that very short intermolecular distances between the interacting dyes (or dyes and quenchers) are required for these emission modulation mechanisms to take place, which we intended to control by selecting appropriate PCMs and concentrations as to warrant: (a) large

separation distances in the liquid state of the system, which in combination with the relatively high viscosity of most melted PCMs and the short lifetime of the singlet excited state of the chromophores should inhibit AIE, ACQ and PET regardless of molecular diffusion; and (b) dye (or dye-quencher) aggregation due to reduced solubility in the solid state of the material, thus facilitating the intermolecular interactions accounting for fluorescence variation (Figure 3a).

**- Insert Figure 3 here -**

After some experimental optimisation, all these effects could indeed be observed when thermally-inducing the solid-to-liquid transition of the following dye solutions in PCMs: **TPE** (0.5 wt%) in eicosane (EC, $T_m$ = 36.5 ºC [60]), **RhB** (2.5 wt%) in TdOH ($T_m$ = 37.7 ºC [60]), and **PTDI** (2.8 $10^{-3}$ wt%) and **DMA** (0.1 wt%) in octacosane (OC, $T_m$ = 61.3 ºC [60]). These mixtures were prepared with PCMs of different $T_m$ and nature to prove that the optical changes observed were only dependent on their solid-to-liquid transition. For all these samples, monomer-like absorption spectra were registered for the fluorophores in the liquid state that significantly broadened and/or shifted upon PCM solidification (Figure S5). These are clear indications of selective dye aggregation in the solid state,[63] though in the case of **PTDI** spectral changes could also originate from the variation of the twisting angle θ between its two naphthalene monoimide units with the rigidity of the environment (Scheme S1).[64] In addition, concomitant changes in fluorescence intensity were observed when cooling down the system below $T_m$, which are consistent with the activation of the AIE, ACQ and PET processes as a result of molecular aggregation and, for the first time, demonstrate the capacity to control these luminescence switching mechanisms using PCMs and readily available dyes (Figure 3b and Table S1). Thus, the strong **TPE** emission registered in solid EC ($\lambda_{em,max}$ = 445 nm) was nearly quantitatively lost upon melting ($\Delta F$ = -98.5%), which we ascribed to selective AIE upon PCM crystallisation. For **RhB** in TdOH, the opposite situation was observed since ACQ is the main mechanism governing the photophysical behaviour of the system when solid, as corroborated

by the dim fluorescence signal determined at 25 ºC. As such, a dramatic enhancement in emission was measured when dissolving the aggregates by melting the PCM matrix ($\lambda_{em,max}$ = 579 nm, $\Delta F$ = +691%). A similar effect was encountered for the mixture of **PTDI** and **DMA** in OC, whose fluorescence intensity strikingly increased when heating above $T_m$ ($\lambda_{em,max}$ = 592 nm, $\Delta F$ = +4641%). However, this result could not be ascribed to ACQ, as intense red-shifted **PTDI** fluorescence was measured in solid OC in the absence of **DMA**, which could be attributed to highly emissive *J*-aggregates[63] and/or variation of the internal twisting angle of isolated dye molecules[64] (Figure S6). Therefore, PET-induced fluorescence quenching arising from selective **PTDI**-**DMA** interaction in the solid state should account for the emission modulation measured in this case. It must be noted that such an heteroaggregation-based effect is unprecedented and, more importantly, that it opens the door for the preparation of thermofluorescent materials[65] from almost any emitter of interest by simple mixture with an appropriate additive (e.g., a PET quencher) in PCMs.

Encouraged by these excellent results, we explored the viability of developing NIR-responsive thermofluorochromic materials based on **TPE**/EC, **RhB**/TdOH and **PTDI**/**DMA**/OC mixtures. With this aim, we prepared porous cellulose-based papers loaded with AuNSs as well as the PCM mixtures described above. The resulting **TPE/EC-AuNS@paper**, **RhB/TdOH-AuNS@paper** and **PTDI/DMA/OC-AuNS@paper** samples preserved the thermal properties of the impregnated PCMs (Figure S7), whose solid-to-liquid transition was attempted optically under NIR illumination at room temperature ($\lambda_{exc}$ = 830 nm, 10.6 mW mm$^{-2}$). As shown in Figures 3c and 3d, Figure S8 and Videos S2, S3 and S4, this led to reversible, repetitive and large fluorescence changes around the irradiated areas that were in agreement with the behaviour observed macroscopically when thermally heating. Hence, clear-cut on-off emission switching was measured for **TPE/EC-AuNS@paper** upon NIR irradiation ($\Delta F$ = -92.3%), while off-on fluorescence modulation was registered for **RhB/TdOH-AuNS@paper** ($\Delta F$ = 620%) and even **PTDI/DMA/OC-AuNS@paper** despite the

significantly higher $T_m$ value of OC ($\Delta F$ = 744%, Table S1). Since no NIR-induced effects were observed for the same samples in the absence of AuNSs (Figure S9), we could assign these results to the dissociation of the emissive **TPE** and quenched **RhB** and **PTDI**/**DMA** aggregates upon local photothermally-induced PCM melting. In addition, NIR-induced fluorescence modulation was found to take place and recover in the dark very rapidly in our samples (i.e., within a few seconds), thus overcoming the slow response rate that often suffer photoswitchable luminescent solid materials based on T-type photochromes owing to matrix effects.

The successful results obtained for the different PCM-dye mixtures analysed herein prove the general applicability of our strategy toward solid materials with NIR-induce fluorescence modulation, a behaviour that is accomplished without the need of NIR-absorbing photochrome-based systems requiring complex syntheses and/or low-probability multiphoton excitation processes. Furthermore, our approach could be potentially broadened to an even larger range of emitters and fluorescence modulation phenomena relying on reversible interchromophoric interactions (e.g., excimer formation[43,45]). Consequently, facile tuning of the emission colour (e.g., from blue **TPE** to reddish **PTDI** fluorescence) and switching scheme of the resulting materials (e.g., on-off or off-on) could be achieved by simply varying the dye of choice, as already demonstrated.

**2.3 Tuneability of the NIR-induced photothermal response of PCM-based thermofluorochromic materials.** After proving that NIR-responsive thermofluorochromic systems could be obtained with the strategy proposed in this work, we then analysed the effect of the variation of some of the key elements that control the material response: the amount of local heat photothermally generated and the PCM melting temperature. The former can be regulated by means of different experimental parameters, such as the concentration of photothermal nanoheaters and the NIR light power density.

To assess the influence of nanoheater concentration and irradiation power, additional experiments were conducted. For this, we first prepared several **RhB/OA-AuNS@paper** samples with decreasing concentration of AuNSs from 13 μg $cm^{-2}$ to 0.8 μg $cm^{-2}$. Two main effects were observed on the resulting NIR-induced off-on fluorescence modulation that we attributed to lower photothermal heating and, as such, reduced PCM solid-to-liquid conversion efficiencies (Figure S10a). On one hand, inferior emission enhancements were determined, which suggests that smaller regions of the sample were photothermally melted. Actually, when excessively diminishing the amount of photothermal nanoheaters ($c_{AuNS}$ = 0.8 μg $cm^{-2}$), no fluorescence increase could be detected upon NIR irradiation. On the other hand, longer illumination times were required to reach constant fluorescence modulation amplitude, although in all the cases this was achieved within few seconds ($t$ < 10 s). As expected, analogous results were obtained when decreasing the NIR excitation intensity for a fixed concentration of AuNSs (13 μg $cm^{-2}$) and, indeed, a threshold power density value was also found (9.4 mW $mm^{-2}$) below which PCM melting could not be achieved and, therefore, no emission switching could be observed (Figure S10b).

The effect of the $T_m$ of the PCM on the NIR-induced fluorescence change response was also analysed. With this aim, we prepared porous cellulose-based papers impregnated with the same amount of AuNSs (13 μg $cm^{-2}$) and **RhB**, but using PCMs of increasing $T_m$ values: TdOH ($T_m$ = 37.7 ºC [60]; **RhB/TdOH-AuNS@paper**), dodecanoic acid (DA, $T_m$ = 43.8 ºC [60]; **RhB/DA-AuNS@paper**) and octadecanoic acid (OA, $T_m$ = 69.3 ºC [60]; **RhB/OA-AuNS@paper**) (Figure S11). In all the cases, large and reversible NIR-induced fluorescence changes were accomplished, which demonstrates the capacity to photothermally melt even high-$T_m$ PCMs at relatively low loadings of metal nanostructures (Table S1). In addition, negligible differences were observed on the rate of the NIR-induced fluorescence increase, most probably due to the great amount of photothermal heat produced very rapidly at the experimental $c_{AuNSs}$ and NIR power conditions used (Figure S12). However, the amplitude of

the fluorescence modulation obtained was found to correlate with the $T_m$ of the PCM at equivalent irradiation conditions. Thus, higher fluorescence increments were achieved for cellulose papers made of PCM-based mixtures of lower melting points, which we attributed to the higher volumes of molten PCM generated photothermally.

In light of the results described above, multithreshold materials that yield several emitting colour states when submitted to NIR radiation of different powers could be accomplished by combining suitable mixtures of PCMs and dyes. To prove this concept, we loaded a cellulose-based paper with AuNSs (13 μg $cm^{-2}$) and then impregnated this substrate with: (a) **TPE** in OC ($T_m$ = 61.3 ºC [60]), which should undergo AIE-based fluorescence on-off switching upon PCM melting; and (b) **RhB** dispersed in a lower-$T_m$ PCM (DA, $T_m$ = 43.8 ºC [60]), which should experience ACQ-induced fluorescence off-on switching when heating. An intercalating poly(vinyl alcohol) (PVA) layer was also introduced to ensure separation of both dye-loaded PCMs, which preserved their different melting temperatures in the final material (Figure 4a and Figure S13). By regulating the NIR irradiation power density, we were able to reversibly measure three distinct emission signals under a single excitation wavelength ($\lambda_{exc}$ = 355 nm) for this sample (Figure 4b). First, blue **TPE** fluorescence was registered in the dark at room temperature where both PCMs lay in the solid state. Next, purple emission arising from mixed blue **TPE** and reddish **RhB** fluorescence was registered at low NIR excitation intensities that selectively led to DA photothermal melting and, as such, redissolution of the quenched **RhB** aggregates (9.4 mW $mm^{-2}$). Finally, only red **RhB** fluorescence was detected when further increasing NIR irradiation power (23.7 mW $mm^{-2}$), which also induced OC solid-to-liquid transition and, hence, disaggregation of the emissive **TPE** assemblies. Therefore, by exploiting the versatility of the PCM-based strategy introduced in this work, single wavelength, NIR-controllable multistate luminescent behaviours can be accomplished from commercially-available fluorophores in a simple manner that could hardly be reached otherwise.

**- Insert Figure 4 here -**

## 2.4 Control of the time response in NIR-writable devices based on photothermofluorochromic materials

To take advantage of the photothermofluorochromic materials developed herein for the fabrication of functional devices showing NIR-induced fluorescence modulation, their time response must fulfil the requirements needed for each application. While fast onset of the luminescence change upon NIR irradiation should in principle be necessary in all the cases, the time it takes to recover the initial fluorescence state after NIR illumination ceases must be fine-tuneable and adaptable to the final use. For this reason, we developed different strategies to obtain fast-, slow- and non recovering (i.e., irreversible) NIR-responsive luminescent materials (Figure 5).

*Thermofluorochromic materials with fast NIR-induced responses.* All the examples of PCM-based thermofluorochromic materials shown above present fast onset and recovery of NIR-induced fluorescence modulation (i.e., within seconds). In spite of this, fine and wide-range tuning of the recovery response was obtained without chemical modification of the dye by simply employing PCMs of different $T_m$, a behaviour that is normally difficult to accomplish in solid materials using T-type photochrome-based switches. This situation is illustrated by the measurements taken on **RhB/OA-AuNS@paper**, **RhB/DA-AuNS@paper** and **RhB/TdOH-AuNS@paper**, which recovered the initial fluorescent state in *ca*. 4 s, *ca.* 10 s and *ca*. 23 s after NIR irradiation, respectively (Figures 5a and 5c). Clearly, faster deactivation kinetics were measured for higher-$T_m$ PCMs, as expected since liquid-to-solid conversion for these materials takes place at higher temperatures that are more rapidly reached during the cooling process. This rapid thermal recovery is reminiscent of the fluorescence modulation effects accomplished with fast-responsive T-type photochromes and could find use in (bio)imaging (e.g., in super-

resolution microscopy[19]), logic gates, signal communication and dynamic anti-counterfeiting technologies based on time-dependent codes.[21]

*Thermofluorochromic materials with slow NIR-induced responses.* For other applications, however, much slower deactivation kinetics after NIR irradiation would be preferred, thus leading to fluorescence changes that are preserved in the dark for prolonged periods of time (e.g. rewritable devices, anti-counterfeiting inks[23]). To achieve this goal, we explored the use of PCMs suffering from strong supercooling effects when solidifying from the melt at room temperature. This is the case of tricaprin, a lipid with $T_m$ = 31.5 ºC that shows a very slow crystallisation rate due to the lack of nucleation centres when cooled down below its melting temperature.[66] Actually, when registering the thermogram of this compound by DSC at regular temperature scan rates (10 ºC $min^{-1}$), solidification was only observed to occur well below $T_m$ (0.1 ºC, Figure S14a). When loading porous cellulose papers with AuNSs, tricaprin, **PTDI** and **DMA** (**PTDI/DMA/tricaprin-AuNS@paper**), this did not prevent observing large and fast fluorescence enhancements upon NIR irradiation (or thermal heating) that were similar to those measured for **PTDI/DMA/OC-AuNS@paper** ($\Delta F$ > 2000%, Table S1 and Figures S14b-S14d).

**- Insert Figure 5 here -**

However, much slower emission deactivation was subsequentially registered due to supercooling effects and, indeed, complete recovery of the initial fluorescence signal at room temperature required more than 60 min for **PTDI/DMA/tricaprin-AuNS@paper** (Figure 5b and Figures S14c and S14d).

Such a dramatic extension of the lifetime of the light-generated fluorescent features allowed us the preparation of self-erasable fluorescent inks responding to invisible NIR

irradiation, a much desired property for rewritable devices and security printing.[25] In the simplest case, this was achieved by irradiation of **PTDI/DMA/tricaprin-AuNS@paper** with a NIR source, either directly or through a mask, where the fluorescent motifs would be merely light-printed (Figure 14e). However, in a much more elaborated operation mode, NIR illumination could be used to visualise previously deposited structures of dye-PCM mixtures and/or photothermal nanoheaters. We validated this idea by creating defined patterns of AuNSs onto porous cellulose paper by inkjet printing, which were then covered with a continuous layer of tricaprin loaded with **PDTI** and **DMA**. Whereas such patterns were invisible under ambient or UV light (Figure S14f), they selectively and precisely turned fluorescent when scanning the whole sample with NIR radiation as to locally melt the PCM and, as such, switch on **PTDI** emission on the areas printed with AuNSs (Figures 5d and S14g, and Video S5). In all cases the developed fluorescent images were retained for several hours before self-erasing.

*Thermofluorochromic materials with irreversible NIR-induced responses.* In some cases, irreversible NIR-induced fluorescent patterns must be needed to be printed onto surfaces. To reach this objective, we explored the use of polymer-based temperature-threshold fluorescent materials that undergo irreversible luminescent changes upon reaching their glass-transition temperature ($T_g$).[65,67,68] Thus, when combined with the photothermal effects produced by AuNSs, this behaviour should allow for irreversible NIR-induced luminescence modulation. As a proof of concept, we used **RhB**/**DA**-containing poly(methyl methacrylate) (PMMA) nanoparticles (**RhB/DA/PMMA_NPs**), a nanostructured temperature-threshold fluorescent material previously developed in our group.[42] These nanoparticles are not fluorescent at room temperature due to ACQ of the RhB molecules, while they turn irreversibly fluorescent when heated above 120 ºC and quickly cooled at room temperature. To transfer this behaviour into a solid macroscopic material, the nanoparticles were deposited onto a porous cellulose paper in the presence of AuNSs, thus yielding a homogeneously coloured and non fluorescent substrate

(**RhB/DA/PMMA_NPs-AuNSs@paper**, Figure S15a). As expected, the fluorescence of this material enhanced irreversibly ($\Delta F$ = 656%) once externally heated up to 120 ºC (Figure S15b). Upon NIR irradiation, a local luminescent spot ($\Delta F$ =1568%) was rapidly developed (Figure S15c), suggesting that the nanoheaters photothermally heated the nanoparticles above PMMA $T_g$. This was also confirmed by SEM analysis, which showed the loss of the spherical shape of **RhB/DA/PMMA_NPs** in the irradiated region (Figure S16). Interestingly, the fluorescence signal was retained after turning the NIR source off, even after several months. As such, this strategy for irreversible fluorescence development is suited for the preparation of permanent NIR-writable fluorescent patterns and substrates for high-resolution NIR-based photothermal printing, which represents a more straightforward alternative to current thermal printing techniques.[69] By simply varying the NIR beam spot size, power and scanning time, we were able to create fluorescent motifs with line thicknesses (i.e. drawing resolution) that could be precisely tuned between ~ 60 μm-200 μm. This would therefore allow the fabrication of high-resolution barcodes of interest for security ink packaging (Figures 5e-f and S17).

## 3. Conclusions

In summary, we reported in this work a conceptually novel strategy to achieve NIR-induced fluorescence modulation in solid materials that relies on two main principles: (a) the capacity of phase change materials to reversibly alter the optical properties of molecular emitters upon solid-liquid transition, and (b) the photothermal heating generated by NIR-absorbing plasmonic nanostructures to induce PCM melting (e.g. gold nanoshells). Multiple advantages derive from this approach. First, our strategy directly applies to readily available, unfunctionalised emitters and PCMs, thus preventing the tedious synthesis of complex photoresponsive molecules such as NIR-absorbing photochromes. Second, by using noble metal nanostructures as NIR absorbers, their stimulation can be decoupled from emitter excitation to minimise photodegradation and destructive readout, while larger NIR-induced responses with lower

irradiation intensities can be generated. As a consequence, very small amounts of these nanostructures are needed to produce substantial photoinduced effects, thus having minimal impact on the emission of the nearby fluorophores and the cost of the final material. In addition, our methodology is highly versatile, as it can make use of a large number of emitters and operate under multiple fluorescence modulation mechanisms deriving from phase-controlled dye-PCM, dye-dye and even dye-additive interactions (e.g., fluorescent molecular rotors, AIE, ACQ, photoinduced electron transfer). This, together with the accurate tuning of some key experimental parameters (e.g., PCM melting temperature, NIR irradiation intensity), allows fine time and amplitude control of the NIR-induced responses as well as the realisation of multithreshold modulation schemes that go beyond single colour on-off or off-on switching. We successfully demonstrated the versatility of this approach to fabricate thermofluorescent materials undergoing fast, slow and irreversible NIR-response, allowing writing patterns of high and controllable resolution. Finally, macroscopic, nanostructured and inkjet-patterned NIR-responsive thermofluorochromic materials can be obtained in this way, thereby paving the way for the preparation of a wide variety of functional materials with applications ranging from (bio)imaging to security printing and sensing.

## 4. Experimental section

The materials, the preparation and characterization methods as well as the supplementary tables, figures and schemes can be found in the supplementary information.

## Supporting Information.

Supporting Information is available from the Wiley Online Library or from the author.

## Acknowledgment

This work was supported by the Spanish Research Agency (AEI) and European Regional Development Funds (CTQ2015-65439-R and RTI2018-098027-B-C21 projects) and Generalitat de Catalunya (2017 SGR00465 project). ICN2 is funded by the CERCA programme (Generalitat de Catalunya) and acknowledges support from the Severo Ochoa programme (AEI, SEV-2017-0706). J. R. O. thanks the Generalitat de Catalunya (AGAUR) for his predoctoral FI fellowship.

**References**


[1] H. Dürr, H. Bouas-Laurent, *Photochromism: Molecules and Systems*, Elsevier Science, Amsterdam, **2003**.

[2] B. L. Feringa, W. R. Browne, *Molecular Switches*, Wiley-VCH, **2011**.

[3] B. M. Russew, S. Hecht, **2010**, 3348.

[4] J. Zhang, Q. Zou, H. Tian, *Adv. Mater.* **2013**, *25*, 378.

[5] S. Mura, J. Nicolas, P. Couvreur, *Nat. Mater.* **2013**, *12*, 991.

[6] M. I. Khazi, W. Jeong, J. M. Kim, *Adv. Mater.* **2018**, *30*, 1705310.

[7] V. Blanco, D. A. Leigh, V. Marcos, *Chem. Soc. Rev.* **2015**, *44*, 5341.

[8] W. Szymański, J. M. Beierle, H. A. V. Kistemaker, W. A. Velema, B. L. Feringa, *Chem. Rev.* **2013**, *113*, 6114.

[9] I. Yildiz, E. Deniz, F. M. Raymo, *Chem. Soc. Rev.* **2009**, *38*, 1859.

[10] Y. Zhang, K. Zhang, J. Wang, Z. Tian, A. D. Q. Li, *Nanoscale* **2015**, *7*, 19342.

[11] D. Kim, S. Y. Park, *Adv. Opt. Mater.* **2018**, *6*, 1.

[12] T. Fukaminato, S. Ishida, R. Métivier, *NPG Asia Mater.* **2018**, *10*, 859.

[13] M. Irie, T. Fukaminato, T. Sasaki, N. Tamai, T. Kawai, *Nature* **2002**, *420*, 759.

[14] S. Kim, S.-J. Yoon, S. Y. Park, *J. Am. Chem. Soc.* **2012**, *134*, 12091.

[15] J. Andréasson, U. Pischel, *Chem. Soc. Rev.* **2015**, *44*, 1053.

[16] G. Naren, C.-W. Hsu, S. Li, M. Morimoto, S. Tang, J. Hernando, G. Guirado, M. Irie, F. M. Raymo, H. Sundén, J. Andréasson, *Nat. Commun.* **2019**, *10*, 3996.

[17] L. Zhu, W. Wu, M.-Q. Zhu, J. J. Han, J. K. Hurst, A. D. Q. Li, *J. Am. Chem. Soc.* **2007**, *129*, 3524.

[18] M. Li, J. Zhao, H. Chu, Y. Mi, Z. Zhou, Z. Di, M. Zhao, L. Li, *Adv. Mater.* **2019**, *31*, 1804745.

[19] P. Dedecker, J. Hofkens, J. Hotta, *Mater. Today* **2008**, *11*, 12.

[20] D. Kim, K. Jeong, S. Y. Park, H. Park, S. Lee, S. Kim, *Nat. Commun.* **2019**, 1.

[21] T. Jiang, Y. F. Zhu, J. C. Zhang, J. Zhu, M. Zhang, J. Qiu, *Adv. Funct. Mater.* **2019**, *29*, 1.

[22] Q. Qi, C. Li, X. Liu, S. Jiang, Z. Xu, R. Lee, M. Zhu, B. Xu, W. Tian, *J. Am. Chem. Soc.* **2017**, *139*, 16036.

[23] H. Wu, Y. Chen, Y. Liu, *Adv. Mater.* **2017**, *29*, 1.

[24] M.-Q. Zhu, G.-F. Zhang, C. Li, M. P. Aldred, E. Chang, R. A. Drezek, A. D. Q. Li, *J. Am. Chem. Soc.* **2011**, *133*, 365.

[25] P. Kumar, S. Singh, B. K. Gupta, *Nanoscale* **2016**, *8*, 14297.

[26] K. Mutoh, M. Sliwa, E. Fron, J. Hofkens, J. Abe, *J. Mater. Chem. C* **2018**, *6*, 9523.

[27] Q. Yu, X. Su, T. Zhang, Y. M. Zhang, M. Li, Y. Liu, S. X. A. Zhang, *J. Mater. Chem. C* **2018**, *6*, 2113.

[28] J. L. Wang, Q. Liu, Y. S. Meng, X. Liu, H. Zheng, Q. Shi, C. Y. Duan, T. Liu, *Chem. Sci.* **2018**, *9*, 2892.

[29] D. Bléger, S. Hecht, *Angew. Chemie - Int. Ed.* **2015**, *54*, 11338.

[30] M. Dong, A. Babalhavaeji, C. V. Collins, K. Jarrah, O. Sadovski, Q. Dai, G. A. Woolley, *J. Am. Chem. Soc.* **2017**, *139*, 13483.

[31] K. Klaue, Y. Garmshausen, S. Hecht, *Angew. Chemie - Int. Ed.* **2018**, *57*, 1414.

[32] P. Lentes, E. Stadler, F. Röhricht, A. Brahms, J. Gröbner, F. D. Sönnichsen, G. Gescheidt, R. Herges, *J. Am. Chem. Soc.* **2019**, *141*, 13592.

[33] J. R. Hemmer, S. O. Poelma, N. Treat, Z. A. Page, N. D. Dolinski, Y. J. Diaz, W. Tomlinson, K. D. Clark, J. P. Hooper, C. Hawker, J. Read de Alaniz, *J. Am. Chem. Soc.* **2016**, *138*, 13960.

[34] M. Izquierdo-Serra, M. Gascón-Moya, J. J. Hirtz, S. Pittolo, K. E. Poskanzer, È. Ferrer, R. Alibés, F. Busqué, R. Yuste, J. Hernando, P. Gorostiza, *J. Am. Chem. Soc.* **2014**, *136*, 8693.

[35] G. Cabré, A. Garrido-Charles, M. Moreno, M. Bosch, M. Porta-de-la-Riva, M. Krieg,

M. Gascón-Moya, N. Camarero, R. Gelabert, J. M. Lluch, F. Busqué, J. Hernando, P. Gorostiza, R. Alibés, *Nat. Commun.* **2019**, *10*, 907.

[36] C. J. Carling, J. C. Boyer, N. R. Branda, *J. Am. Chem. Soc.* **2009**, *131*, 10838.

[37] S. Wu, H. J. Butt, *Adv. Mater.* **2016**, *28*, 1208.

[38] S. Chen, A. Z. Weitemier, X. Zeng, L. He, X. Wang, Y. Tao, A. J. Y. Huang, Y. Hashimotodani, M. Kano, H. Iwasaki, L. K. Parajuli, S. Okabe, D. B. Loong Teh, A. H. All, I. Tsutsui-Kimura, K. F. Tanaka, X. Liu, T. J. McHugh, *Science (80-. ).* **2018**, *359*, 679.

[39] J. Moreno, M. Gerecke, L. Grubert, S. A. Kovalenko, S. Hecht, *Angew. Chemie - Int. Ed.* **2016**, *55*, 1544.

[40] H. Sotome, T. Nagasaka, K. Une, C. Okui, Y. Ishibashi, K. Kamada, S. Kobatake, M. Irie, H. Miyasaka, *J. Phys. Chem. Lett.* **2017**, *8*, 3272.

[41] G. Massaro, J. Hernando, D. Ruiz-Molina, C. Roscini, L. Latterini, *Chem. Mater.* **2016**, *28*, 738.

[42] A. Julià López, D. Ruiz-Molina, K. Landfester, M. B. Bannwarth, C. Roscini, *Adv. Funct. Mater.* **2018**, *28*, 1.

[43] G. Massaro, G. Zampini, D. Ruiz-Molina, J. Hernando, C. Roscini, L. Latterini, *J. Phys. Chem. C* **2019**, *123*, 4632.

[44] Y. J. Jin, R. Dogra, I. W. Cheong, G. Kwak, *ACS Appl. Mater. Interfaces* **2015**, *7*, 14485.

[45] J. Du, L. Sheng, Q. Chen, Y. Xu, W. Li, X. Wang, M. Li, S. X. Zhang, *Mater. Horizons* **2019**, DOI: 10.1039/c9mh00253g.

[46] Y. J. Jin, Y. G. Choi, H. Park, G. Kwak, *J. Mol. Liq.* **2018**, *265*, 260.

[47] W. Zhang, X. Ji, B. Peng, S. Che, F. Ge, W. Liu, M. Al-Hashimi, C. Wang, L. Fang, *Adv. Funct. Mater.* **2020**, *30*, 1906463.

[48] J. Liu, C. Detrembleur, M.-C. De Pauw-Gillet, S. Mornet, C. Jérôme, E. Duguet, *Small*

**2015**, *11*, 2323.

[49] M. Wu, Y. Shi, R. Li, P. Wang, *ACS Appl. Mater. Interfaces* **2018**, *10*, 39819.

[50] Y. Zhang, M. M. Umair, S. Zhang, B. Tang, *J. Mater. Chem. A* **2019**, *7*, 22218.

[51] P. K. Jain, X. Huang, I. H. El-Sayed, M. A. El-Sayed, *Acc. Chem. Res.* **2008**, *41*, 1578.

[52] M. Herder, B. M. Schmidt, L. Grubert, M. Pätzel, J. Schwarz, S. Hecht, *J. Am. Chem. Soc.* **2015**, *137*, 2738.

[53] M. Berberich, A. Krause, M. Orlandi, F. Scandola, F. Würthner, **2008**, 6616.

[54] D. Su, C. L. Teoh, L. Wang, X. Liu, Y.-T. Chang, *Chem. Soc. Rev.* **2017**, *46*, 4833.

[55] L. R. Hirsch, R. J. Stafford, J. A. Bankson, S. R. Sershen, B. Rivera, R. E. Price, J. D. Hazle, N. J. Halas, J. L. West, *Proc. Natl. Acad. Sci.* **2003**, *100*, 13549.

[56] E. R. Evans, P. Bugga, V. Asthana, R. Drezek, *Mater. Today* **2018**, *21*, 673.

[57] Y. Guan, Z. Xue, J. Liang, Z. Huang, W. Yang, *Colloids Surfaces A Physicochem. Eng. Asp.* **2016**, *502*, 6.

[58] E. E. Nesterov, J. Skoch, B. T. Hyman, W. E. Klunk, B. J. Bacskai, T. M. Swager, *Angew. Chemie Int. Ed.* **2005**, *44*, 5452.

[59] F. Peccati, J. Hernando, L. Blancafort, X. Solans-Monfort, M. Sodupe, *Phys. Chem. Chem. Phys.* **2015**, *17*, 19718.

[60] D. R. Lide, *CRC Handbook of Chemistry and Physics*, CRC Press, Boca Raton, FL, **2016**.

[61] H. Wang, E. Zhao, J. W. Y. Lam, B. Z. Tang, *Mater. Today* **2015**, *18*, 365.

[62] L. Zang, R. Liu, M. W. Holman, K. T. Nguyen, D. M. Adams, *J. Am. Chem. Soc.* **2002**, *124*, 10640.

[63] M. Kasha, H. R. Rawls, M. Ashraf El-Bayoumi, *Pure Appl. Chem.* **1965**, *11*, 371.

[64] M. Streiter, S. Krause, C. von Borczyskowski, C. Deibel, *J. Phys. Chem. Lett.* **2016**, *7*, 4281.

[65] A. Seeboth, D. Lötzsch, R. Ruhmann, O. Muehling, *Chem. Rev.* **2014**, *114*, 3037.

[66] K. Sato, Ed. , *Crystallization of Lipids: Fundamentals and Applications in Food, Cosmetics, and Pharmaceuticals*, Wiley Blackwell, **2018**.

[67] M. Kinami, B. R. Crenshaw, C. Weder, *Chem. Mater.* **2006**, *18*, 946.

[68] B. R. Crenshaw, C. Weder, *Adv. Mater.* **2005**, *17*, 1471.

[69] L. Chen, M. Weng, F. Huang, W. Zhang, *ACS Appl. Mater. Interfaces* **2018**, *10*, 40149.

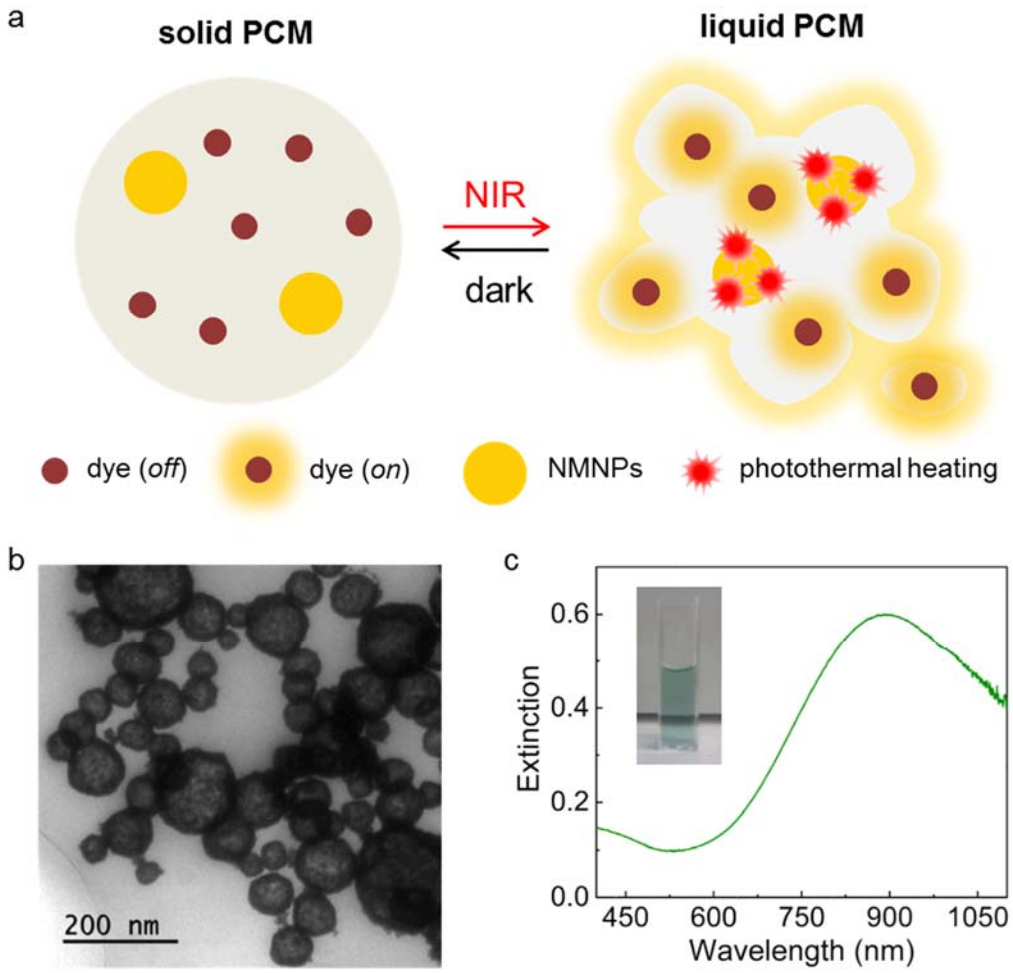


**Figure 1.** (a) NIR-induced fluorescence modulation in thermofluorochromic materials based on emitters, PCMs and metal nanoparticles. By inducing PCM melting via the photothermal effects generated by NMNPs under NIR irradiation, the properties of the dissolved dyes vary and a change in fluorescence emission is produced (as example the fluorescence modulation from the *off* to the *on* state is illustrated, though the opposite case, i.e. from *on* to *off*, is also verified). The description "dye (*off*)" and "dye (*on*)", indicates any situation where the dye molecule is in its non-fluorescent or fluorescent state, respectively, as consequence of the PCM phase change, regardless the mechanism involved in the fluorescence enhancement/quenching transition (*vide infra*). When NIR illumination is stopped, PCM solidification occurs and the initial emissive behaviour is recovered. (b-c) TEM image and extinction spectrum in water of the AuNSs used in this work as NIR-excitable nanoheaters. The inset in (c) shows a photograph of an aqueous AuNS suspension (22 μg $mL^{-1}$).

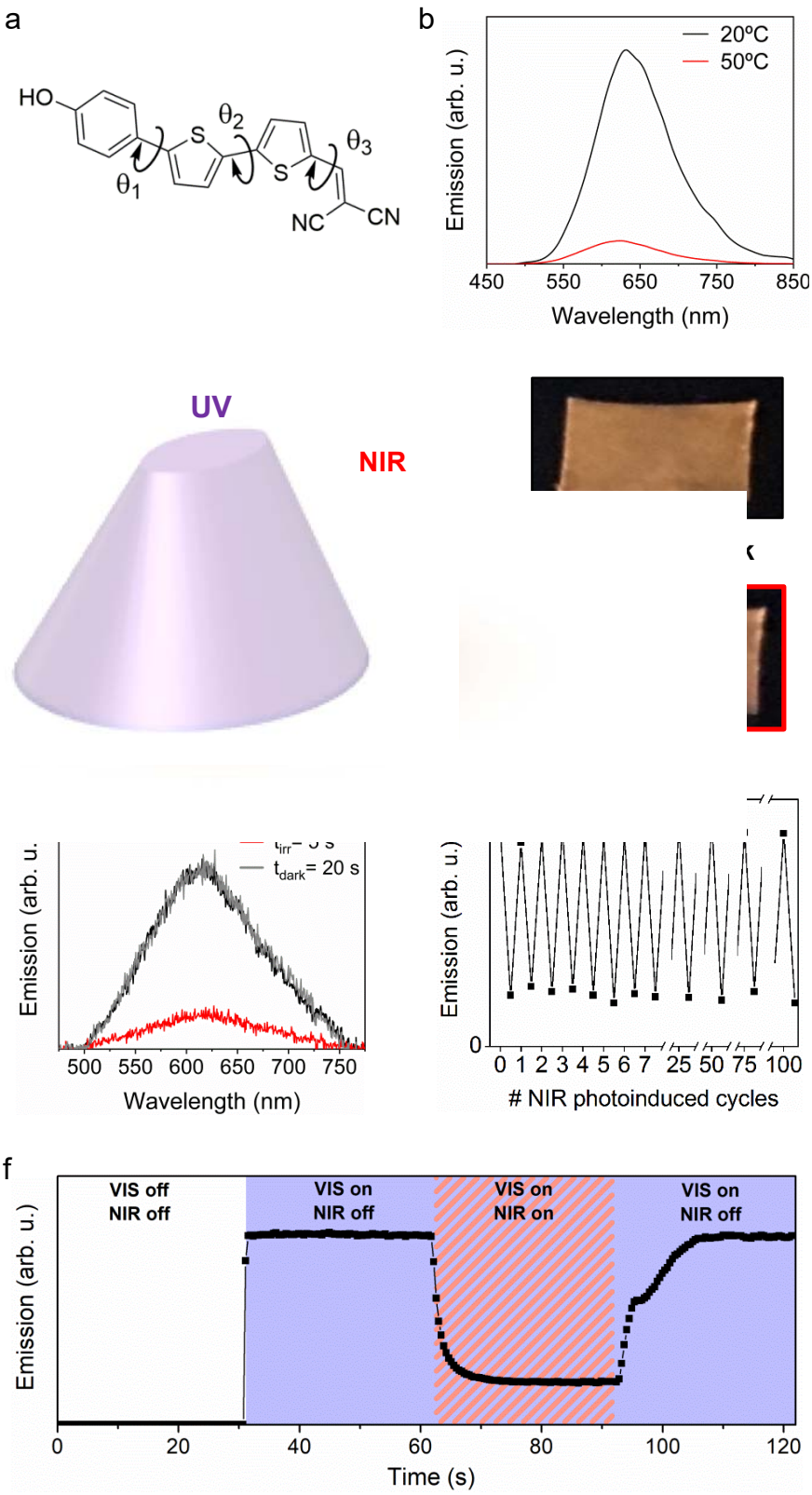


**Figure 2.** (a) Structure of **NIAD-4**, which can undergo intramolecular rotations through dihedral angles $\theta_1$, $\theta_2$ and $\theta_3$. (b) Emission spectra ($\lambda_{exc}$ = 445 nm) of **NIAD-4** in TdOH (2.4 $10^{-3}$ wt%) at 20 °C (solid state) and 50 °C (liquid state). (c) Irradiation with a cw NIR laser on a local spot ($\lambda_{exc}$ = 830 nm, 10.6 mW $mm^{-2}$) allows selective deactivation of the fluorescence emitted by **NIAD-4/TdOH-AuNS@paper** under UV illumination ($\lambda_{exc}$ = 365 nm). Photographs of **NIAD-4/TdOH-AuNS@paper** before and after local NIR excitation are shown.

(d) Emission spectra ($\lambda_{exc}$ = 445 nm) of a local spot of **NIAD-4/TdOH-AuNS@paper** before ($t_0$), during ($t_{irr}$ = 5 s) and after ($t_{dark}$ = 20 s) NIR light irradiation. (e) Variation in emission intensity ($\lambda_{exc}$ = 445 nm) on a local spot of **NIAD-4/TdOH-AuNS@paper** after consecutive cycles of NIR photoexcitation. (f) Variation in emission intensity on a local spot of **NIAD-4/TdOH@paper** by switching on and off the **NIAD-4** excitation ($\lambda_{exc}$ = 445 nm, VIS) and NIR illumination ($\lambda_{exc}$ = 830 nm and 10.6 mW mm$^{-2}$, NIR) sources.

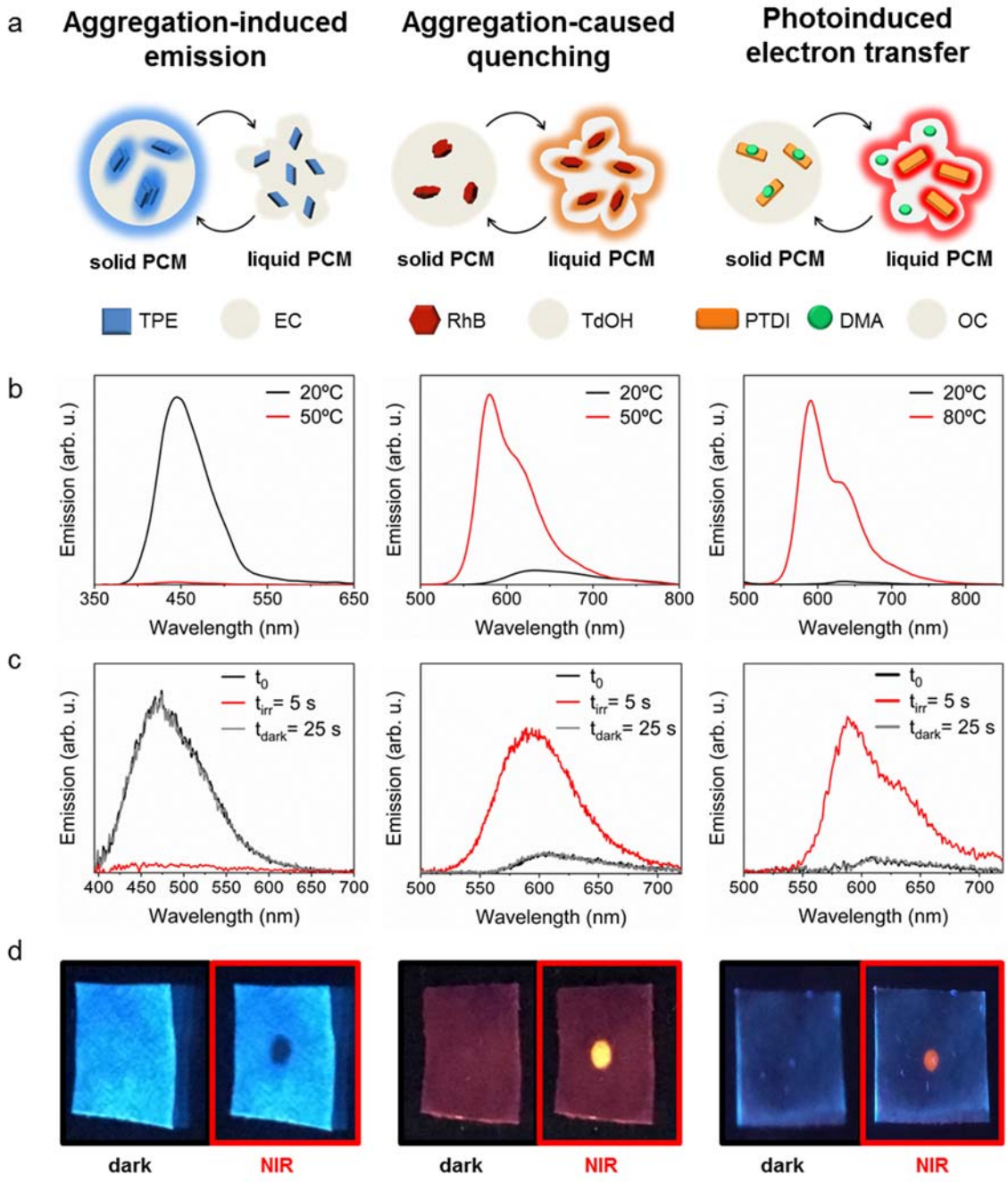


**Figure 3.** (a) Scheme of the phase-controlled photophysical and photochemical processes exploited to achieve fluorescence modulation with **TPE**, **RhB** and **PTDI**: aggregation-induced emission (**TPE**), aggregation-caused quenching (**RhB**) and photoinduced electron transfer (**PTDI**), which are selectively induced in the solid state of the PCM. (b) (left to right) Emission spectra of **TPE** in EC, **RhB** in TdOH and a mixture of **PTDI** and **DMA** in OC at 20ºC and after thermal heating to induce EC (50ºC), TdOH (50ºC) and OC (80ºC) melting. (c) (left to right)

Emission spectra of a local spot of **TPE/EC-AuNS@paper** ($\lambda_{exc}$ = 355 nm), **RhB/TdOH-AuNS@paper** ($\lambda_{exc}$ = 405 nm) and **PTDI/DMA/OC-AuNS@paper** ($\lambda_{exc}$ = 445 nm) before ($t_0$), during ($t_{irr}$ = 10 s) and after ($t_{dark}$ = 25 s) NIR light irradiation ($\lambda_{exc}$ = 830 nm, 10.6 mW mm$^{-2}$). (d) (left to right) Photographs of the emission from these samples ($\lambda_{exc}$ = 365 nm) with and without local NIR irradiation. Clearly, selective fluorescence deactivation (**TPE/EC-AuNS@paper**) or activation (**RhB/TdOH-AuNS@paper** and **PTDI/DMA/OC-AuNS@paper**) is achieved on the illuminated spot, thus leading to on-off or off-on NIR-induced emission modulation, respectively.

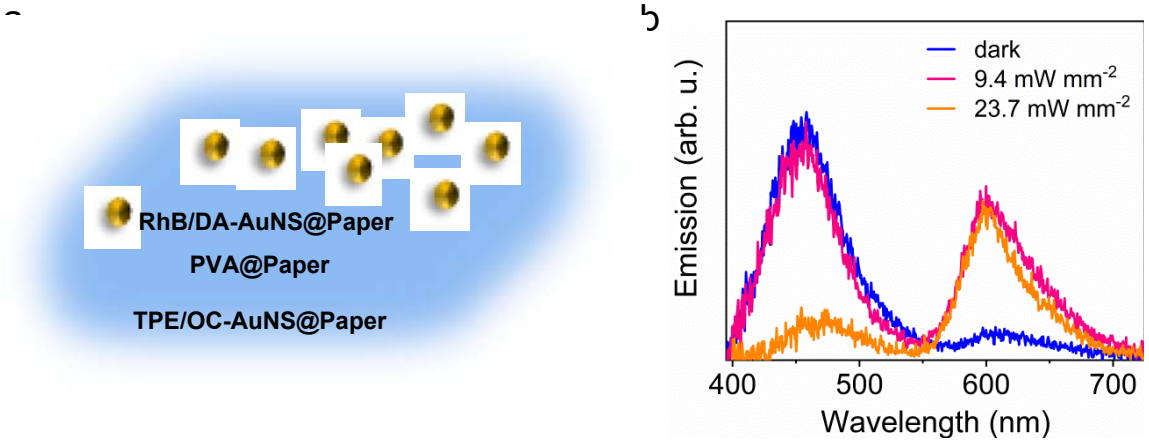


**Figure 4**. (a) Scheme of the three-colour emitting material made by impregnation of an AuNS-loaded cellulose paper with consecutive **TPE**/OC, PVA and **RhB**/ DA layers. (b) NIR-triggered variation of the emission arising from this material ($\lambda_{exc}$ = 355 nm for fluorescence excitation; $\lambda_{exc}$ = 830 nm for NIR irradiation at 9.4 or 23.7 mW mm$^{-2}$).

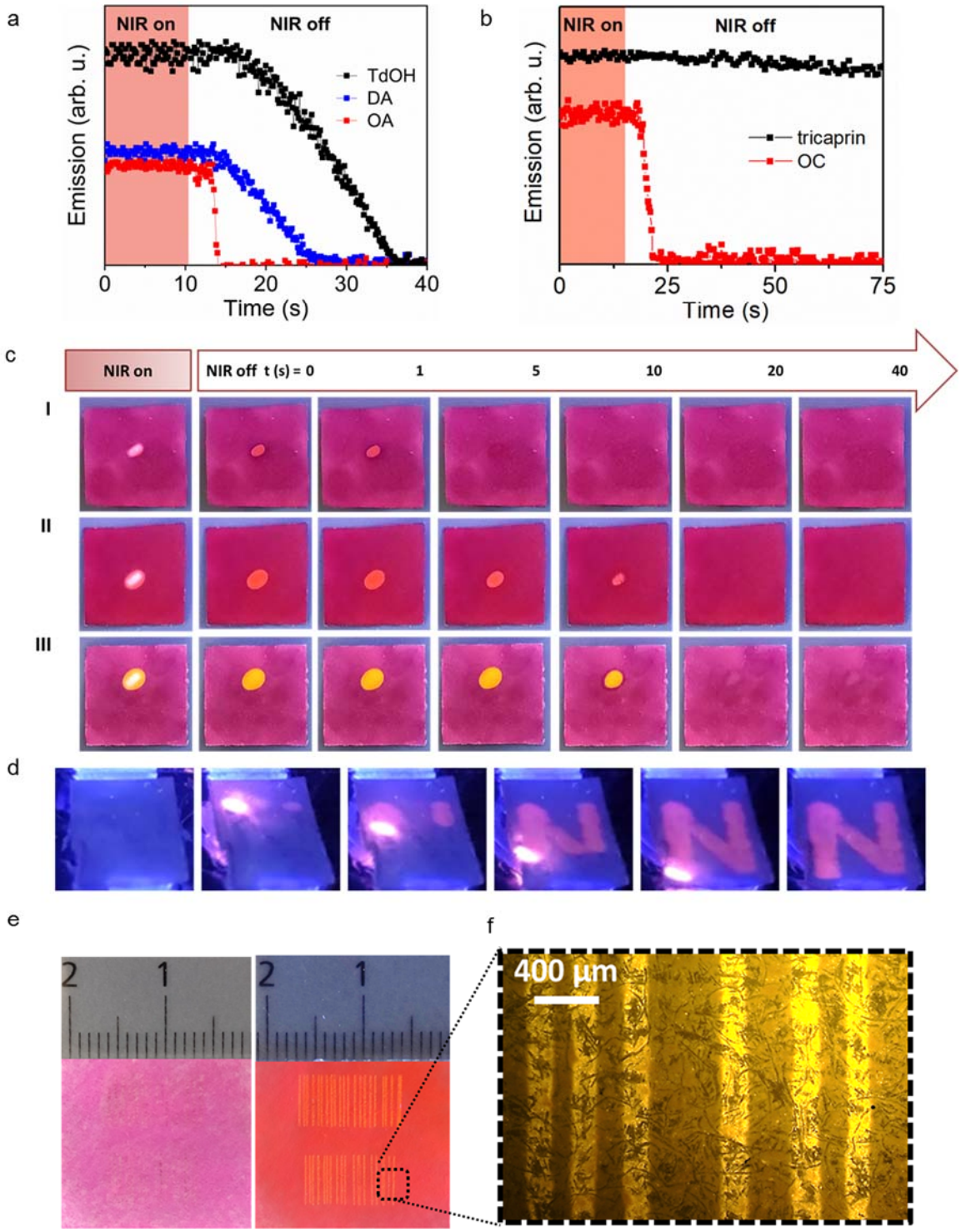


**Figure 5.** Recovery kinetics in the dark, at room temperature, of the emission of (a) **RhB/TdOH-AuNS@paper**, **RhB/DA-AuNS@paper**, and **RhB/SA-AuNS@paper** ($\lambda_{exc}$ = 405 nm, $\lambda_{em}$ = 600 nm, $c_{AuNS}$ = 13 µg cm$^{-2}$, NIR power = 23.7 mW mm$^{-2}$) and of (b) **PTDI/DMA/tricaprin-AuNS@paper** and **PTDI/DMA/OC-AuNS@paper** ($c_{AuNS}$ = 13 µg cm$^{-2}$, $\lambda_{exc}$ = 445 nm, $\lambda_{em}$ = 600 nm) after NIR-induced activation at 830 nm (10.6 mW mm$^{-2}$). (c) Snapshots of the decrease of the emission of **RhB/OA-AuNS@paper** (I), **RhB/DA-AuNS@paper** (II), and **RhB/TdOH-AuNS@paper** (III) obtained under UV illumination ($\lambda_{exc}$ = 365 nm), in the dark and room temperature after irradiation with NIR. (d) Snapshots obtained under UV illumination ($\lambda_{exc}$ = 365 nm) showing the development of a fluorescent letter by scanning a NIR beam ($\lambda_{exc}$ = 830 nm, 10.6 mW mm$^{-2}$) all over a **PTDI/DMA/tricaprin-**

**AuNS@paper** sample prepared with an inkjet-printed pattern of AuNSs. (e) Photographs under ambient light, and UV illumination of **RhB/DA/PMMA_NPs-AuNSs@paper**, where permanent fluorescent lines of different thickness were directly written by moving the sample holder at different speeds (5-25 mm/s) while irradiating with the NIR beam ($\lambda_{exc}$ = 830 nm, 93.5 mW $mm^{-2}$). (f) Fluorescence microscopy image under UV illumination ($\lambda_{exc}$ = 365 nm) of the locally NIR-irradiated ($\lambda_{exc}$ = 830 nm, 93.5 mW $mm^{-2}$, 7.5 mm/s) **RhB/DA/PMMA_NPs-AuNSs@paper**.

**Table of contents**

Herein it is reported a new, straightforward and photochrome-free strategy to obtain luminescent materials, whose fluorescence can be modulated by near infrared radiation (NIR). This approach allows obtaining solid cellulose-based papers which, upon low-intense NIR irradiation, self-erasing or permanent drawings (e.g. barcodes), are easily obtained in very good resolution.

**Keyword** luminescence modulation

*Jaume Ramon Otaegui, Pau Rubirola, Daniel Ruiz-Molina, Jordi Hernando,* and Claudio Roscini**

**Solid Materials with Near-Infrared-Induced Fluorescence Modulation**